Vol 17 No 10, October 2008
1674-1056/2008/17(10)/3812-10

Chinese Physics B

© 2008 Chin. Phys. Soc.
and IOP Publishing Ltd

Bridge density functional approximation for non-uniform hard core repulsive Yukawa fluid*

Zhou Shi-Qi(周世琦)

School of Physics Science and Technology, Central South University, Changsha 412008, *China*

(Received 6 July 2007; revised manuscript received 8 February 2008)

In this work, a bridge density functional approximation (BDFA) (*J. Chem. Phys.* **1**12, 8079 (2000)) for a non-uniform hard-sphere fluid is extended to a non-uniform hard-core repulsive Yukawa (HCRY) fluid. It is found that the choice of a bulk bridge functional approximation is crucial for both a uniform HCRY fluid and a non-uniform HCRY fluid. A new bridge functional approximation is proposed, which can accurately predict the radial distribution function of the bulk HCRY fluid. With the new bridge functional approximation and its associated bulk second order direct correlation function as input, the BDFA can be used to well calculate the density profile of the HCRY fluid subjected to the influence of varying external fields, and the theoretical predictions are in good agreement with the corresponding simulation data. The calculated results indicate that the present BDFA captures quantitatively the phenomena such as the coexistence of solid-like high density phase and low density gas phase, and the adsorption properties of the HCRY fluid, which qualitatively differ from those of the fluids combining both hard-core repulsion and an attractive tail.

Keywords: bridge density functional approximation, radial distribution function, colloid, density distribution

PACC: 6000, 6120J

1. Introduction

Non-uniform fluids consisting of particles interacting through a hard-core repulsion and an attractive tail, are extensively investigated theoretically, numerically and experimentally as well.[1] One of the theoretical tools, the density functional theory (DFT) approach, is developed greatly due to the experience based on the investigation of these potentials, the density functional approximation (DFA) for potentials combining both a hard-core repulsion and an attractive tail originating from the extension of hard-sphere DFA.[2] Far less investigated are the purely repulsive potentials which exist as a model of potentials for real fluids. Some of examples include an inverse power potential, a core-softened potential, a penetrable-sphere potential, a purely repulsive Coulomb potential, a Gaussian core potential, a hard-core repulsive Yukawa (HCRY) potential, etc. All of these potentials can be good representative of some real fluids. For example, the purely repulsive Coulomb potential represents a simplest model of the potential for charged point particles immersed in a uniform neutralized background;[3] the Gaussian core potential is usually used to represent the entropic repulsion between the centres-of-mass of self-avoiding polymer coils dispersed in a good solvent;[4] the penetrable-sphere potential is usually considered as a prototype of the interaction between micellae in a solvent;[5] the core-softened potential is employed to explain the anomalous property of water, liquid metals under specific conditions;[6] the HCRY potential can be used to model a structure and thermodynamic properties of charged colloidal particles immersed in an electrolyte water solution.[7] Taking into account the generality of the purely repulsive potentials in modelling real fluids, it is very important to formulate DFAs for these purely repulsive potentials which display properties different from those shown by the potentials including the attractive tail as well as the hard core. Singly using one of the most successful hard-sphere DFAs, i.e. the fundamental-measure functional (FMF),[8] is not sufficient for describing the non-hard-sphere potentials. The reason lies in its close connection with the employment of geometrical measures of the hard sphere in its construction. Here, by 'singly' the author means the fact that in order to describe the non-hard-sphere potentials the FMF has to combine with other approximations, such as the mean field approximation, for the perturbation

*Project supported by the National Natural Science Foundation of China (Grant No 20673150).

tail. So our attention will be paid to another successful hard-sphere DFA, the bridge density functional approximation (BDFA).[9] The BDFA is very successful for calculating the density profile[9] and surface tension[10] of non-uniform hard-sphere fluid, also it is the simplest, in the sense of computation, among all existing successful DFAs.[2] Its computational cost is equal to that for using a second order functional perturbation expansion approximation (FPEA)[11] which however is only qualitatively correct for a non-uniform hard-sphere fluid. At present, the BDFA is successful only in the application to a non-uniform single-component hard-sphere fluid,[9,10,12] a non-uniform binary hard-sphere fluid.[13,14] and a non-uniform hard-sphere chain fluid.[15] By employing specially-devised bridge functional approximation, the BDFA can also be successfully applied to a non-uniform sticky hard-sphere fluid and a penetrable-sphere fluid.[16,17] However, the straightforward extension of the hard-sphere BDFA to non-uniform penetrable-sphere fluids by employing the Percus–Yevick (PY) approximation for the bridge function is only partially successful.[18] It was shown in Ref.[18] that the BDFA based on the PY approximation held true only for the case of high temperatures, while the FMF[8] was sufficient only for the case of low temperatures. For the non-uniform Lennard-Jones fluid whose interparticle potential includes both the hard core repulsion and the attractive tail, even if one employed the specially-devised bridge function approximation,[19,20] the BDFA was also only partially successful; In fact, it fails for the cases of low temperatures and low densities.[20] By employing the BDFA for treating the hard core part of the non-hard-sphere interaction potential, the BDFA also finds its successful application to a non-uniform electrolyte solution (i.e. electrical double layer).[21] and a non-uniform sticky hard-sphere fluid.[22] From all of these applications of the BDFA cited above, one can conclude that the BDFA is a popular, very convenient DFA in use, and has a potential of widespread applications in liquid physics. However, its successful application in liquid physics depends on the employment of an appropriate bridge functional approximation. Philosophy of the BDFA is as follows: the bulk bridge functional should be expressed as a function of bulk indirect correlation function (ICF); and then by making use of the Ornstein–Zernike (OZ) integral equation (IE), the ICF is rewritten as a convoluted integral involving the density profile (bulk radial distribution function is exactly equal to the density profile divided by the bulk density) and bulk second order direct correlation function (DCF); the resulting expression is also applicable to the non-uniform case because of universality of the free energy density functional[23] and its first order functional derivative.[9] For potentials with an attractive tail, the bridge functional cannot be expressed as a function of the ICF, but it can be written as a function of a renormalized ICF.[24] Therefore, it is not surprising that the BDFA is not directly suitable for these fluids over the whole density range.[20] However, for purely repulsive potentials, the bridge functional is not so weird that it can be expressed as a function of the ICF. This opens up possibilities for the straightforward extension of the BDFA to these purely repulsive potentials. The aim of the present report is to explore in detail the possibilities, and propose a new bulk bridge functional approximation applicable for both the bulk HCRY model fluid and for non-uniform HCRY model fluid as input into the BDFA reformulated.

The rest of the present paper is organized as follows. In Section 2 we propose a new bridge functional approximation whose validity for the bulk HCRY model fluid is tested by comparing the resultant bulk fluid radial distribution function (RDF) with corresponding recently proposed simulation data[25] in Section 3. Then, in Section 3, we introduce the new bridge functional approximation and its associated bulk second order DCF into the BDFA and calculate the density profile of the HCRY model fluid subjected to the influence of varying external fields, thereby making a comprehensive comparison between the present density profile and corresponding simulation data.[25] The adsorption behaviours of the HCRY fluid are also investigated by employing the present BDFA in Section 3. Finally, in Section 4, we give a detailed discussion about the present work.

2. Bridge density functional approximation for inhomogeneous HCRY fluids

Adopted in this work is the intermolecular potential, i.e. the HCRY potential, which is given by

$$\beta u(r) = \begin{cases} \infty, & r/\sigma < 1, \\ \beta\varepsilon\sigma \exp[-\kappa^*(r-\sigma)/\sigma]/r, & r/\sigma > 1, \end{cases} \quad (1)$$

where ε and σ are energy and length scales of the potential; the absolute temperature T is in reduced units, i.e. $T^* = kT/\varepsilon$, with k being the Boltzmann constant; κ^* is the reduced screening parameter which dominates over the range of the HCRY potential.

Two key inputs necessary for the BDFA are the bulk second order DCF $C_0^{(2)}(r;\rho_{\rm b}\ldots)$ of high accuracy and an appropriate bulk bridge functional approximation $B[\gamma(r)]$ as a function of the bulk ICF $\gamma(r)$, where $\rho_{\rm b}\ldots$ denotes a set of bulk parameters and $\rho_{\rm b}$ is the bulk density. For the former quantity, we have tried several available bridge functions or bridge functional approximations in combination with the OZ IE. And we find that classical approximations such as the PY approximation, hypernetted chain approximation (HNC) and Rogers–Young approximation[26,27] cannot hold true for the whole parameter space. Especially, the performance for high bulk density $\rho_{\rm b}$ is very bad, or the physical solution at high bulk densities even cannot be found at all. An exception is a semi-empirical parametrized bridge function given by Malijevsky and Labik[28] which holds for the HCRY potential. However, in the Malijevsky–Labik (ML) empirical approximation the bridge function is expressed as a function of particle separation. Although it is useful for obtaining the bulk $C_0^{(2)}(r;\rho_{\rm b}\ldots)$ numerically, it is not suitable as the bridge functional approximation used in the BDFA. If one employs the ML bridge function approximation to obtain the bulk $C_0^{(2)}(r;\rho_{\rm b}\ldots)$, then one has to choose an additional bridge functional approximation as input into the BDFA. For self-consistency, we will propose a new bridge functional approximation used for both obtaining the bulk $C_0^{(2)}(r;\rho_{\rm b}\ldots)$ and implementing the BDFA.

Our new bridge functional approximation is based on the well-known BPGG approximation,[29]

$$B_{\rm BPGG}(\gamma) = (1+s\gamma)^{1/s} - 1 - \gamma, \tag{2}$$

where $s = 15/8$. The present bridge functional approximation is in the following form:

$$B_{\rm M-BPGG}(\gamma) = \begin{cases} -0.5\gamma^2, & \gamma \le 0, \\ (1+s\gamma)^{1/s} - 1 - \gamma, & \gamma \ge 0. \end{cases} \tag{3}$$

There exist two differences between the present approximation and the BPGG approximation. The first difference is that for the negative argument, we specify the approximation as $-0.5\gamma^2$ instead of the original mathematical form, which is based on two considerations: one is that the original form possibly becomes meaningless mathematically when γ becomes negative, the other is that the resulting new form produces more accurate predictions for density profile as shown later in the paper. The second difference is that the present exponent s is adjustable, not fixed at 15/8 but it is fixed in the BPGG approximation. Its explanation will be given later.

One of the input parameters, i.e. the bulk $C_0^{(2)}(r;\rho_{\rm b}\ldots)$, is obtained by solving the OZ IE Eq.(4) combined with the bridge functional approximation Eq.(3) used in the closure equation Eq.(5)

$$\begin{aligned} & h(r) - C_0^{(2)}(r;\rho_{\rm b}\ldots) \\ &= \rho_{\rm b}\int {\rm d}r_1 h(r_1) C_0^{(2)}(|r-r_1|;\rho_{\rm b}\ldots), \end{aligned} \tag{4}$$

$$h(r) + 1 = \exp\left\{-\beta u(r) + \gamma + B(r)\right\}, \tag{5}$$

where, $\gamma(r) = h - C_0^{(2)}(r;\rho_{\rm b}\ldots)$ is the so-called ICF cited above, $h(r) = g(r) - 1$ is the so-called total correlation function, $g(r)$ is the RDF cited above, and B is the bridge function.

In the BDFA, one specifies the non-uniform first order DCF $C^{(1)}(r;[\rho]\ldots)$ as follows:

$$\begin{aligned} & C^{(1)}(r;[\rho]\ldots) \\ &= C_0^{(1)}(\rho_{\rm b}\ldots) + \int {\rm d}r'[\rho(r') - \rho_{\rm b}] \\ &\quad \times C_0^{(2)}(|r-r'|;\rho_{\rm b}\ldots) \\ &\quad + B\Bigg[\int {\rm d}r'[\rho(\mathbf{r}') - \rho_{\rm b}] \\ &\quad \times C_0^{(2)}(|r-r'|;\rho_{\rm b}\ldots)\Bigg], \end{aligned} \tag{6}$$

where $C_0^{(1)}(\rho_{\rm b}\ldots)$ is the uniform first order DCF, and $\rho(r)$ is the density profile.

Substituting Eq.(6) into a single component density profile Eq.(7) leads to a calculating formalism Eq.(8)

$$\begin{aligned} \rho(r) = \rho_{\rm b}\exp\Big\{ & -\beta\varphi_{\rm ext}(r) + C^{(1)}(r;[\rho]\ldots) \\ & - C_0^{(1)}(\rho_{\rm b}\ldots)\Big\}, \end{aligned} \tag{7}$$

where $\varphi_{\rm ext}(r)$ is an external potential responsible for the generation of the $\rho(r)$,

$$\rho(r) = \rho_{\rm b}\exp\Bigg\{-\beta\varphi_{\rm ext}(r) + \int {\rm d}r'[\rho(r') - \rho_{\rm b}]C_0^{(2)}(|r-r'|\,;\rho_{\rm b}\cdot\cdot) + B\left[\int {\rm d}r'[\rho(r') - \rho_{\rm b}]C_0^{(2)}(|r-r'|\,;\rho_{\rm b}\ldots)\right]\Bigg\}. \quad (8)$$

As far as the specification of exponent s is concerned, although the adjustable parameter s can be determined by thermodynamic self-consistent conditions, we find that for the present application in the BDFA, the specification of s by using the single hard wall sum rule[30] will be more beneficial for the accurate prediction of the $\rho(r)$ as indicated in the present author's previous publication.[31] So, the determined value of s should depend on the bulk parameters such as the $\rho_{\rm b}$, κ^* and T^*. However, we also find that the choosing of $s = 1.5$ is sufficient for both the bulk and the non-uniform HCRY fluids for all of the investigated cases. Thus, in the present paper, $s = 1.5$ is employed.

We will investigate several cases of $\varphi_{\rm ext}(r)$. Besides the single hard wall, we treat also a planar gap, i.e. the two hard walls separated by a distance H, and a spherical cavity surrounded by a spherical hard wall. The external potentials due to the presence of these spatial constrains may be expressed as

$$\varphi_{\rm ext}(z) = \begin{cases} \infty, & z/\sigma < 0.5, \\ 0, & 0.5 < z/\sigma, \end{cases} \quad (9)$$

for the single hard wall;

$$\varphi_{\rm ext}(z) = \begin{cases} \infty, & z/\sigma < 0.5 \ \text{ or } \ z/\sigma > H/\sigma - 0.5, \\ 0, & 0.5 < z/\sigma < H/\sigma - 0.5, \end{cases} \quad (10)$$

for the planar slit with two plane hard walls situated at $z = 0$ and $z = H$, respectively;

$$\varphi_{\rm ext}(r) = \begin{cases} \infty, & r > R, \\ 0, & r < R, \end{cases} \quad (11)$$

for the spherical cavity with the hard spherical wall of an effective radius R.

3. Results and discussion

Since highly accurate bulk $C_0^{(2)}(r;\rho_{\rm b}\ldots)$ is very crucial to any successful DFAs, we first test the accuracy of the present $C_0^{(2)}(r;\rho_{\rm b}\ldots)$ by comparing the associated bulk RDF with the corresponding simulation data[25] in Figs.1 and 2, showing that the present bridge functional approximation Eq.(3) with a fixed value of $s = 1.5$ predicts the bulk RDFs in very good agreement with the simulation data[25] for a wide range of parameters. Therefore one can conclude that Eq.(3) will also predict the bulk $C_0^{(2)}(r;\rho_{\rm b}\ldots)$ very accurately, since both $C_0^{(2)}(r;\rho_{\rm b}\ldots)$ and $g(r)$ are dependent on each other. In Ref.[25], the Grand Canonical Ensemble Monte Carlo (GCEMC) simulations were carried out at a constant chemical potential μ, volume V, and temperature T, this set of independent parameters that determine the thermodynamic state of the system made possible the study of equilibrium between the bulk HCRY fluids with and without being subjected to different external fields originating from the different spatial constrains. Theoretical predictions for $\rho(r)$ of the non-uniform HCRY fluid based on the present BDFA DFT approach and the corresponding simulation data[25] for two sets of bulk parameters are presented in Figs.3–8. These figures show the curves of $\rho(r)$ for the HCRY fluid sequentially: (i) at the single hard wall (Figs.3 and 4), (ii) in the planar gap with a width $H = 3\sigma$ (Figs.5 and 6), and (iii) in the hard spherical cavity with an effective radius $R = 3.5\sigma$ (Figs.7 and 8). To make a comparison between the present approach and the approaches available from the literature, we present in Figs.5 and 6 the predictions by using a DFT approach[32] based on a direct correlation function described in Ref.[33]. For the sake of clarity, the majority of figures are subdivided into two or three parts, which successively illustrate the effect of increase in the bulk density at constant values of potential parameters T^* and κ^*. A comparison between the theoretical predictions and the simulation data[25] for the $\rho(r)$ of the HCRY fluid in various inhomogeneous systems indicates a very good accuracy of the present BDFA DFT approach. An exception to the above observation is an obvious deviation of the theoretical $\rho(r)$ from the simulation result in the region around the centre of the spherical cavity for the highest bulk density considered (Fig.8). However, this disagreement can be ascribed to a low relia-

bility of the simulation data for this regime stemming from poor statistics of this part of data. Namely, the $\rho(r)$ is determined from the average number of the particles found within the spherical shells into which the spherical cavity is subdivided. As the volume of these shells decreases on approaching the centre of the cavity, the counting statistics worsens in the same direction. It should be noted that for the case of the planar slit with two plane hard walls the small disagreement still exists near the middle centre when the bulk density is higher (Figs.5(c) and 6(c)). Considering that so narrow slit constitutes a strong confinement and for the strongly repulsive HCRY fluid, the bulk density of $\rho_{\rm b}\sigma^3 = 0.7$ is not far away from the solid-liquid transition point,[34] the presence of so small deviation is not a surprise. We can therefore conclude that the present theoretical approach is highly reliable for the HCRY fluid in confined systems. From Figs.5 and 6 one finds that the present approach is comparable in accuracy with the approach available from Refs.[32,33].

As reported in numerous articles dealing with the behaviours of fluids at interfaces and in confined systems, a general feature found from the structures of fluids was their spatial nonuniformity as a consequence of the packing effects of fluid molecules in the domain close to the wall. The actual details of the density profiles that characterize this nonuniformity depend on the specific nature of the fluid-fluid and the wall-fluid interactions, and on the degree and geometry of confinement. In this work, various confined geometries have been considered in order to examine how the expressiveness of the 'nonuniformity' of the system affects the quality of the performance of the DFT approach. Since the present calculation refers to the model fluid with purely repulsive interparticle interactions instead of potentials with an attractive tail as well as a hard core repulsion, it is also very interesting to compare the present results with the qualitative features found from the inhomogeneous molecular models that combine both the repulsion and the attraction among the molecules,[35] when, of course, the effect of the same spatial constraints as a source for the external potential is considered in both cases. When an inhomogeneous structure of the fluid stems from the presence of a single wall, the flat density profile of $\rho(z) = \rho_{\rm b}$ is restored at a sufficient distance from the wall, irrespective of the specific nature of the intermolecular potential of interactions. Near the wall these interactions compete with steric effects. This competition, of course, is now strongly dependent on the particular intermolecular potential and on the temperature of the system as well. In any case, the interactions among the molecules gain in importance upon lowering temperature. As the strongly attractive molecules have a better chance for mutual attraction at sufficient distances from the wall or outside the confined system, they are driven away from the hard obstacles or toward the centre of the micro-objects with a restricted geometry (planar gap, spherical cavity).[35] As expected, just the opposite behaviour is observed for the molecules interacting through a purely repulsive interaction potential. Clearly, the strongly repulsive molecules try to avoid each other and as such they prefer the regions adjacent to the walls of the confinement. Such molecules are therefore accumulated near the walls to a greater extent than those due to some attractive interactions, thus giving rise to more pronounced packing effects leading to a more distinct layered structure and a higher wall-fluid contact density

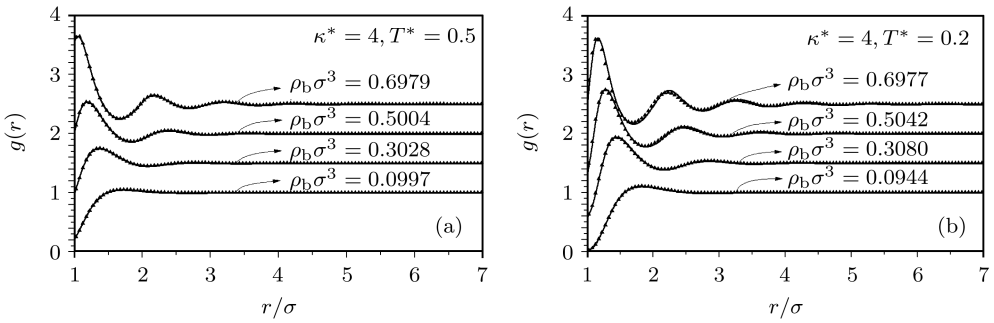


Fig.1. A comparison between the curves of RDF $g(r)$, obtained from the OZ IE theory (lines) based on the present bridge functional approximation and the simulation results[25] (symbols). The bulk parameters are shown in the figures, for the sake of clarity, the data corresponding to individual densities are shifted upwards by different factors (0,0.5, 1,1.5) respectively.

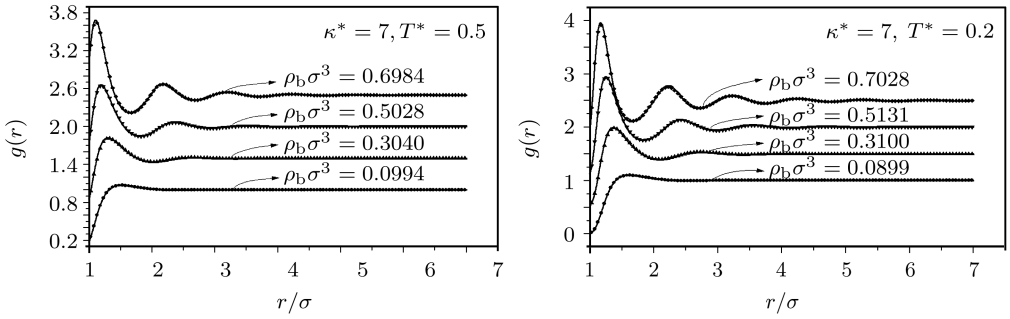


Fig.2. The same caption as that in Fig.1 but for bulk parameters as shown in the figure.

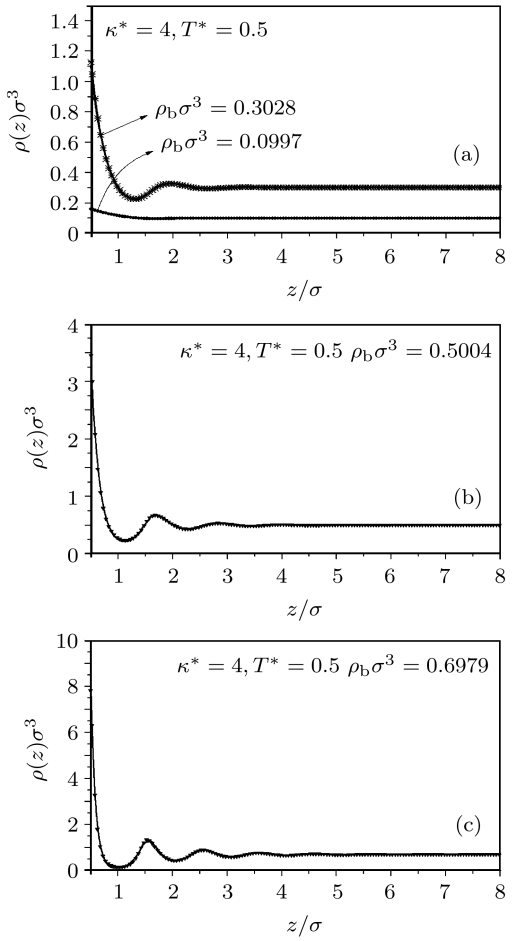


Fig.3. The theoretical results (lines) and simulation results (symbols)[25] for the density profiles of the HCRY fluid at a single hard wall. The bulk parameters are shown in the figure.

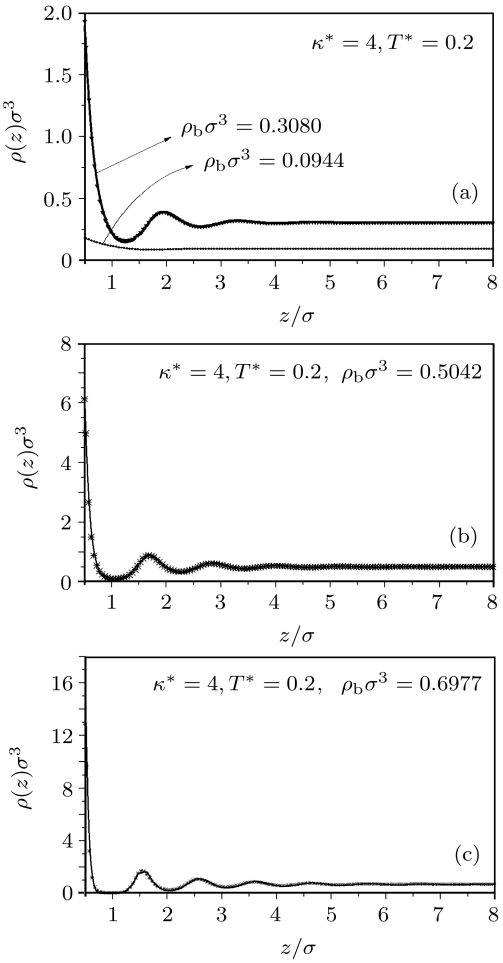


Fig.4. The same caption as that in Fig.3 but for bulk parameters as shown in the figure.

of the fluid with repulsive particles. As mentioned above, the role of the interparticle interactions strengthens with the temperature decreasing. For this reason, lowering temperature causes a reduction in the contact density and weaker oscillations in the density near the wall in the case of the model fluids with attractive molecules.[35] Again, just the opposite case holds for the fluid of our present interest. As clearly seen from the comparisons between Figs.3 and 4 (single wall), between Figs.5 and 6 (planar gap), and between Figs.7 and 8 (spherical cavity), the contact densities (for approximation. the same bulk densities are

adopted here.) are considerably higher at the lower reduced temperature $T^* = 0.2$ (Figs.4, 6, and 8) than those at $T^* = 0.5$ (Figs.3, 5, and 7). To summarize, the imposing of the qualitatively different interactions (attractive or repulsive) on the molecules of the fluid gives rise to qualitatively different redistributions of the molecules inside the confined system, leading to thermodynamically the most favourable structures in both cases.

The effect of temperature is clearly illustrated in Figs.9(a) and 9(b) where the reduced excess adsorption $\Gamma^*_{\rm Ex}$ and the relative reduced excess adsorption $\Gamma^*_{\rm ExRel}$ are presented as a function of the reduced temperature T^* for several different values of $\rho_{\rm b}\sigma^3$, with the relevant parameter and the effective cavity radius being $\kappa^* = 4$ and $R = 3\sigma$, and they are expressed as

$$\Gamma^*_{\rm Ex} = \frac{\int_0^R {\rm d}r 4\pi r^2(\rho(r) - \rho_{\rm b})}{4\pi R^2}, \tag{12}$$

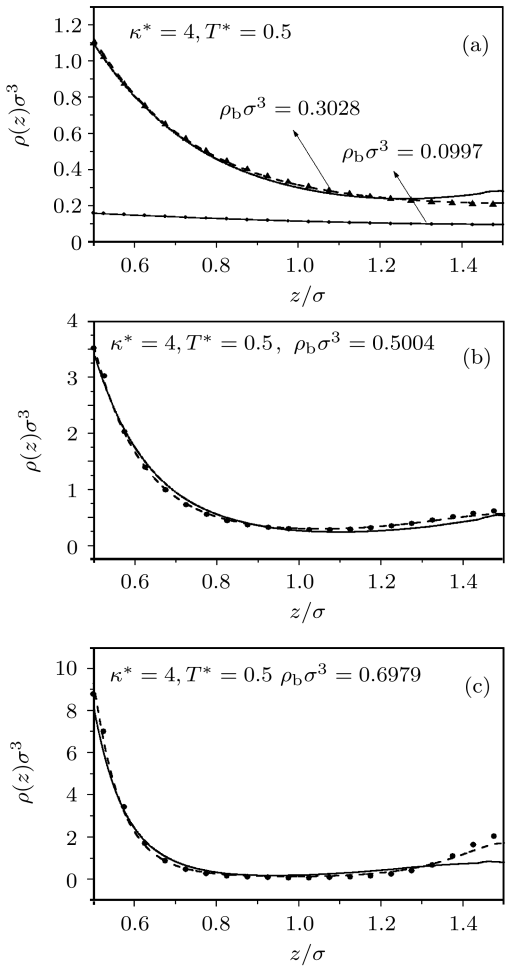


Fig.5. The theoretical results (solid lines for the present approach and dashed lines for the DFT approach in Refs. [32,33]) and simulation results[25] for the density profiles of the HCRY fluid in the gap of width $H = 3\sigma$. The bulk parameters are shown in the figure.

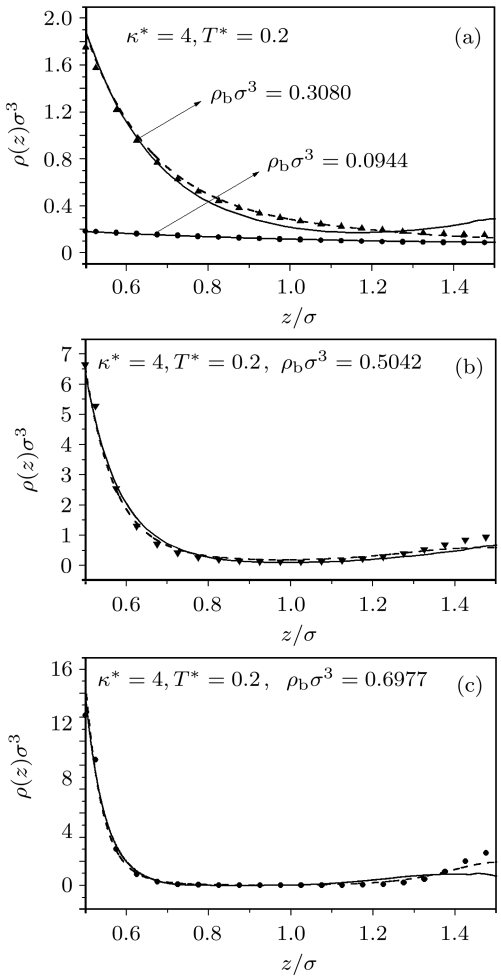


Fig.6. The same caption as that in Fig.5 but for bulk parameters as shown in the figures.

and

$$\Gamma^*_{\rm ExRel} = \frac{\Gamma^*_{\rm Ex}}{(4/3)\pi R^3 \rho_{\rm b}}. \tag{13}$$

An increasing packing effect due to temperature decreasing is reflected as a negative slopes of $\Gamma^*_{\rm Ex}$ versus T^* and $\Gamma^*_{\rm ExRel}$ versus T^*; an increasing bulk density strengthens the packing effect and results in $\Gamma^*_{\rm Ex}$ increasing. We also plot the curve of $\Gamma^*_{\rm ExRel}$ as a function of temperature and bulk density, for the relative quantity more accurately reflects the effect of bulk density. The negative slopes of $\Gamma^*_{\rm Ex}$ versus T^* and $\Gamma^*_{\rm ExRel}$ versus T^* are in contrast to the case of potentials including both the hard core repulsion and the attractive tail, such as LJ fluid confined also in a spherical cavity (see Fig.12 of Ref.[36]). The reason has already been explained above.

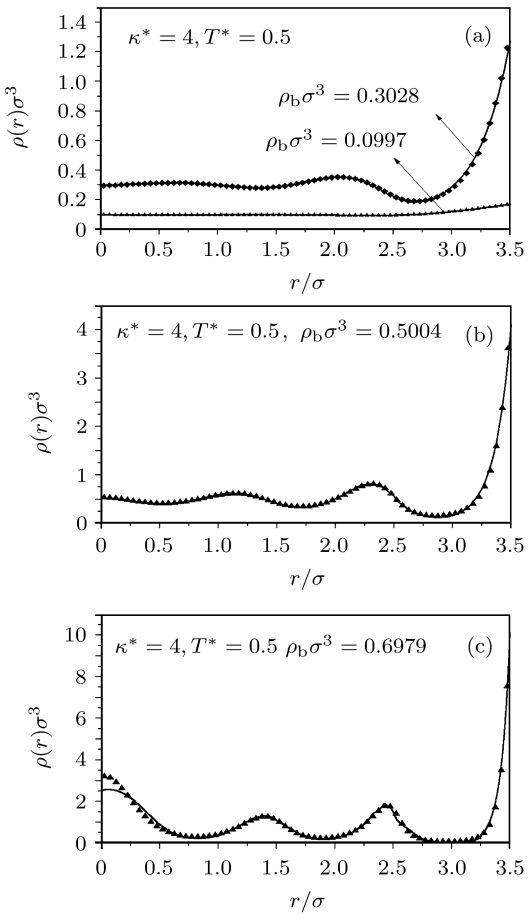


Fig.7. The theoretical results (lines) and simulation results (symbols)[25] for the density profiles of the HCRY fluid in a spherical cavity of radius $R = 3.5\sigma$. The bulk parameters are shown in the figure.

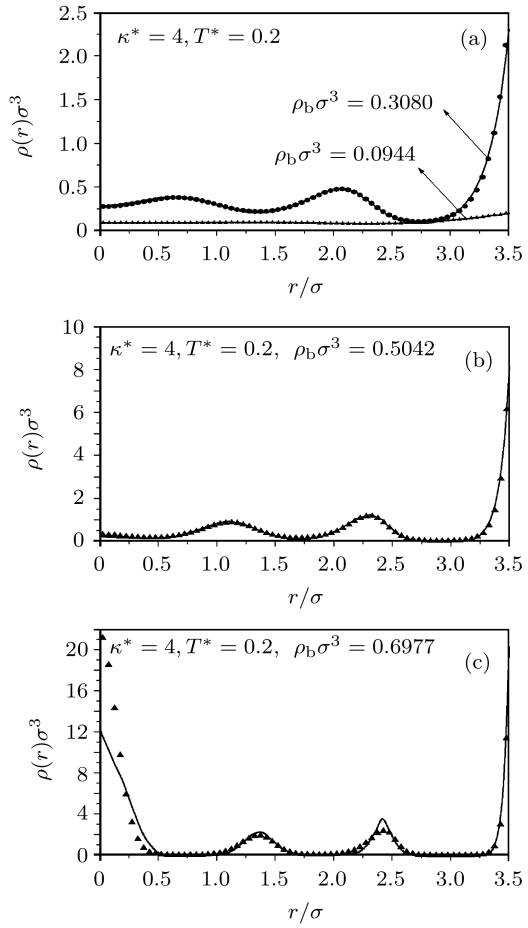


Fig.8. The same caption as that in Fig.7 but for bulk parameters as shown in the figure.

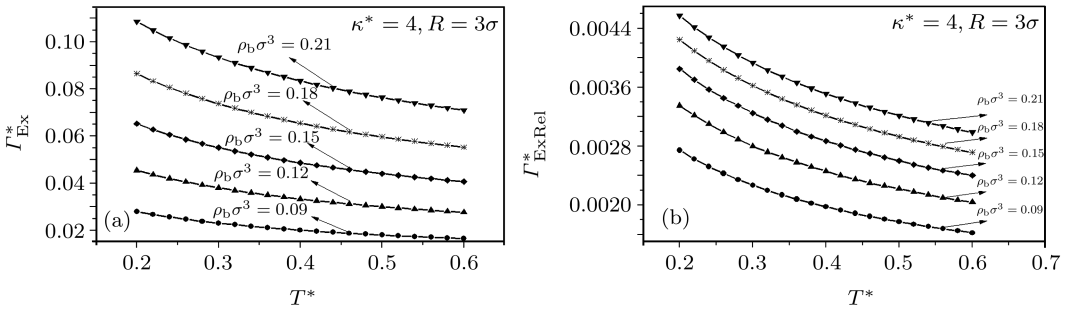


Fig.9. The reduced excess adsorption $\Gamma^*_{\rm Ex}$ (a) and relative reduced excess adsorption $\Gamma^*_{\rm ExRel}$(b) as a function of reduced temperature T^* for a hard spherical cavity of effective radius $R = 3\sigma$. The coexistence bulk density and reduced range parameter are shown in the figure.

It is desirable that our approach very satisfactorily capture the layering transition and the coexistence between high density solid-like phase and low density gas phase in the confined regions. The coexistence originates from the strong packing effect as explained in the followings. The strong packing effect pushes the fluid particle towards the hard wall, and so results in the first high density adsorption layer near the hard wall. The high density adsorption layer forms the first virtual hard wall. It is the virtual hard wall that results successively in the second high density adsorption layer. The intermediate low density gas phase layer is due to the strong repulsion between the HCRY fluid particles and the first virtual hard wall. Since

the density of the first virtual hard wall is lower than that of the spherical hard wall and the particles constituting the first virtual hard wall are subjected to a small repulsion with a range longer than 0.5σ, as well as the particles constituting the second pseudo-hard wall suffer an infinite hard spherical repulsion with a range equal to 0.5σ, the density of the second virtual hard wall is lower than that of the first virtual hard wall. The same reasoning is also applicable to explaining why the density of the low density gas phase layer becomes higher and higher as their position is situated away from the spherical hard wall.

Unlike the case of the potentials with an attractive tail as well as a hard core repulsion where the distance between two neighbouring wave crests or troughs is almost equal to the diameter of the fluid particle, the distance between two neighbouring layers for the case of the HCRY fluid is larger than the diameter of the particles. Since oscillatory density profile reflects the packing effect, the above observation indicates that the effective diameter of the HCRY particle is larger than the diameter of hard core, which obviously conforms to the intuitive consideration.

4. Summary

The present BDFA DFT approach is self-consistent since the bulk $C_0^{(2)}(r;\rho_{\rm b}\ldots)$ and the bridge functional employed in the BDFA result from the same bridge functional approximation Eq.(3). Although a small deviation between the single hard wall contact density and the simulating contact density appears, it can be removed away by employing the single hard wall sum rule for the specification of the adjustable parameter s, the calculations indicate that the resulting values of s for various bulk conditions are all around 1.5.

The BDFA is based on the functional perturbation expansion approximation and summing up all of the higher order terms in the bridge functional approximation. It is a little surprising that the performance as shown in Figs.3(c), 4(c), 5(c), 6(c), 7(c), and 8(c) for highly oscillatory density profile is very good. Such an excellent performance is ascribed to the employment of appropriate bridge functional approximation. It is very interesting to apply the present bridge functional approximation Eq.(3) in combination with the BDFA to other non-uniform purely repulsive potential fluids mentioned in the introduction.

Extension of the present DFT formalism for non-uniform single component HCRY fluid to non-uniform binary HCRY mixture is very straightforward. All one has to do is first specify the adjustable parameters in the bulk bridge functional approximation by using the thermodynamic consistent constraints for bulk fluid, then proceed by following the procedure for non-uniform binary hard sphere mixture,[13] thereby resulting in the DFT formalism for non-uniform binary HCRY mixture. One thing that deserves to be pointed out is that the bulk bridge functional approximation should be expressed as a function of the ICF as done in the present single component formalism.

Since the OZ IE can be numerically solved for purely repulsive fluids over the whole density range, one can numerically obtain the bulk $C_0^{(1)}(\rho_{\rm b}\ldots)$ from zero density to high density, this allows applying the present BDFA DFT approach to investigating the surface tension by using the functional integration method.[10,37] We will investigate in detail the surface tension behaviour of purely repulsive fluids in future reports.

References

[1] Gosselin P and Mohrbach H 2005 *Phys. Rev.* E **71** 031101
Lyklema J 2005 *Phys. Rev.* E **71** 032501
Fleck C C and Netz R R 2005 *Phys. Rev. Lett.* **95** 128101
Paul S and Chandra A 2005 *J. Chem. Phys.* **123** 184706
Sarkisov L and Van Tassel P R 2005 *J. Chem. Phys.* **123** 164706
Becke A D and Johnson E R 2005 *J. Chem. Phys.* **123** 154101
Koga K and Tanaka H 2005 *J. Chem. Phys.* **122** 104711

[2] Henderson D 1992 *Fundamentals of Inhomogeneous Fluids* (New York: Dekker) pp85–176

[3] Baus M and Hansen J P 1980 *Phys. Rep.* **59** 1
Pan C N and Fang M Fa 2008 *Chin. Phys.* B **17** 34
Feng Y L and Shen K 2008 *Chin. Phys.* B **17** 111

[4] Prestipino S, Saija F and Giaquinta P V 2005 *Phys. Rev.* E **71** 050102(R)

[5] Marquest C and Witten T A 1989 *J. Phys.* (France) **50** 1267
Huang Z H, Dong Y L and Wu F 2007 *Chin. Phys.* **16** 2291

[6] Skibinsky A, Buldyrev S V, Franzese G, Malescio G and Stanley H E 2004 *Phys. Rev.* E **69** 061206
Wu F 2007 *Chin. Phys.* **16** 1186

[7] Verwey E J W and Overbeek J T G 1948 *Theory of the Stability of Lyophobic Colloids* (Amsterdam: Elsevier) pp45–67

[8] Rosenfeld Y 1989 *Phys. Rev. Lett.* **63** 980
[9] Zhou S and Ruckenstein E 2000 *J. Chem. Phys.* **112** 8079
[10] Zhou S 2003 *Chin. Phys. Lett.* **20** 2107
[11] Ramakrishnan T V and Yussouff M 1979 *Phys. Rev.* B **19** 2775
[12] Kim M S and Kim S C 2002 *J. Korean Phys. Soc.* **41** 343
Lou Z M 2007 *Chin. Phys.* **16** 1182
[13] Zhou S 2000 *J. Chem. Phys.* **113** 8719
[14] Choudhury N and Ghosh S K 2001 *J. Chem. Phys.* **114** 8530
[15] Zhou S and Zhang X 2001 *Phys. Rev.* E **64** 011112
[16] Zhou S and Zhang X 2002 *Acta Physico-Chimica Sinica.* **18** 699
Zhou S 2007 *Chin. Phys.* **16** 1167
[17] Zhou S 2006 *Commun. Theor. Phys.* (Beijing, China). **46** 323
Zhou S and Zhang X 2002 *Chin. Phys.* **11** 1051
[18] Kim S C and Suh S H 2002 *J. Chem. Phys.* **117** 9880
[19] Zhou S and Ruckenstein E 2000 *J. Chem. Phys.* **112** 5242
[20] Zhou S 2003 *Phys. Rev.* E **68** 061201
Ma H, Tan X, Tian S F, Tong D M and Fan X J 2007 *Chin. Phys.* **16** 2400
[21] Patra C N and Ghosh S K 2002 *J. Chem. Phys.* **117** 8933
[22] Zhou S 2001 *J. Phys. Chem.* B **105** 10360
[23] Chayes J T and Chayes L 1984 *Commun. Math. Phys.* **93** 57
[24] Zerah G and Hansen J P 1986 *J. Chem. Phys.* **84** 2336
Qin Y P 2007 *Chin. Phys.* **16** 3605
[25] Zhou S and Jamnik A 2006 *J. Phys. Chem.* B **110** 6924
[26] Martynov G A 1992 *Fundamental Theory of Liquids. Method of Distribution Functions* (Bristol: Adam Hilger) p34-136
[27] Rogers F J and Young D A 1984 *Phys. Rev.* A **30** 999
[28] Malijevsky A and Labik S 1987 *Mol. Phys.* **60** 663
Li X J 2007 *Chin. Phys.* **16** 2837
[29] Ballone P G, Pastore G, Galli G and Gazillo D 1986 *Mol. Phys.* **59** 275
[30] Henderson J R 1992 *in Fundamentals of Inhomogeneous Fluids* **,** edited by D. Henderson (New York: Dekker) pp23–84
[31] Zhou S 2002 *New J. Phys.* **4** 36
[32] You F Q, Yu Y X and Gao G H 2005 *J. Phys. Chem.* B **109** 3512
[33] Yu Y X, You F Q, Tang Y P, Gao G H and Li Y G 2006 *J. Phys. Chem.* B **110** 334
[34] Hynninen A P and Dijkstra M 2003 *Phys. Rev.* E **68** 021407
Ye S Y 2007 *Chin. Phys.* **16** 2968
[35] Zhou S 2003 *Chem. Phys.* **289** 309
[36] Zhou S 2005 *J. Colloid and Interface Sci.* **290** 364
[37] Zhou S 2004 *Chem. Phys. Lett.* **385** 208